

Cooling of US Midwest summer temperature extremes from cropland intensification

Nathaniel D. Mueller^{1,2*}, Ethan E. Butler^{1,3}, Karen A. McKinnon¹, Andrew Rhines¹, Martin Tingley⁴, N. Michele Holbrook² and Peter Huybers¹

High temperature extremes during the growing season can reduce agricultural production. At the same time, agricultural practices can modify temperatures by altering the surface energy budget. Here we identify centennial trends towards more favourable growing conditions in the US Midwest, including cooler summer temperature extremes and increased precipitation, and investigate the origins of these shifts. Statistically significant correspondence is found between the cooling pattern and trends in cropland intensification, as well as with trends towards greater irrigated land over a small subset of the domain. Land conversion to cropland, often considered an important influence on historical temperatures, is not significantly associated with cooling. We suggest that agricultural intensification increases the potential for evapotranspiration, leading to cooler temperatures and contributing to increased precipitation. The tendency for greater evapotranspiration on hotter days is consistent with our finding that cooling trends are greatest for the highest temperature percentiles. Temperatures over rainfed croplands show no cooling trend during drought conditions, consistent with evapotranspiration requiring adequate soil moisture, and implying that modern drought events feature greater warming as baseline cooler temperatures revert to historically high extremes.

Increasing population, rising per capita food demand, and limited availability of arable land all point to a need to achieve greater crop productivity¹. Climate change, however, may compromise the ability to sustain growth in crop yields², in part owing to expected increases in damaging extreme temperatures^{3–5}. Yet agricultural areas are subject to substantial local, as well as global, climate forcings, as changes in agricultural land cover and land management can alter the surface energy balance and influence temperatures^{6–20}. Against this backdrop, it is relevant to examine historical trends in growing-season climate, especially in the most important growing regions. We focus on the US Midwest because it exhibits the most vigorous crop growth anywhere on the planet during the peak of the growing season (Fig. 1), and because of the availability of detailed weather and crop data.

Centennial trends in Midwest summer climate

Although overall US temperature trends are towards warming over the past century, the hottest temperatures observed during the growing season in the US Midwest have actually cooled. We examine temperature since 1910 as a balance between duration and availability of continuous data, and use quantile regression of daily maximum temperature records from weather stations to assess trends across multiple percentiles (see Methods). Trends in hot summer temperatures are evaluated using the 95th percentile, and are of particular interest because of the negative effects of high temperatures on yield^{3–5}. Midwest cooling is less evident in median temperature trends, and temperatures are generally warming at the 5th percentile (Fig. 2a,b). These trends are robust to the exclusion of the Dust Bowl (1930s), excluding the period of maximum aerosol-induced cooling^{21,22} (1970s–1990s) over the eastern US, and to focusing only on recent decades (for example, 1980–2014, see Supplementary Fig. 1). For purposes of clarity and to maximize our

observational window, we focus on the period 1910–2014, excluding the Dust Bowl and aerosol-induced cooling intervals. A number of other cooling patterns have also been discussed in the literature^{22–26}, but the focus has generally been on other seasons and locations less relevant to agricultural production (further discussion in the Supplementary Information).

Accompanying the decline in extreme temperatures are increases in summer precipitation over much of the upper Midwest (Fig. 2c). Precipitation increases are generally favourable for crop production, notwithstanding damages that can arise from excess moisture. Patterns of increased precipitation and 95th percentile cooling are generally co-located. Stations with precipitation trends greater than 3 mm per decade significantly correspond to regions of cooling ($P < 0.01$, Fig. 2d). Note that significance estimates account for temporal autocorrelation by bootstrapping across years and spatial autocorrelation by resampling each station time series identically.

The question arises as to whether it is merely fortuitous that the climate has become more favourable over the agriculturally dominated Midwest, or whether agricultural land use contributes to the observed trends. Climate models driven by historical forcings generally fail to capture Midwest summer temperature²⁷ and precipitation²⁸ trends, including when observed sea surface temperatures are specified in an attempt to reproduce precipitation patterns. These analyses suggest a possible role for land use change in explaining decreased temperature extremes and increased precipitation during the growing season.

Land conversion to cropland

We first examine whether conversion of natural vegetation to cropland led to cooling. Climate model simulations of land conversion indicate a 0.5–1 °C decrease in mean summer temperatures from increased albedo and crop evapotranspiration⁷.

¹Department of Earth and Planetary Sciences, Harvard University, Massachusetts 02138, USA. ²Department of Organismic and Evolutionary Biology, Harvard University, Massachusetts 02138, USA. ³Department of Forest Resources, University of Minnesota, Minnesota 55108, USA. ⁴Departments of Meteorology and Statistics, The Pennsylvania State University, Pennsylvania 16802, USA. *e-mail: nmueller@fas.harvard.edu

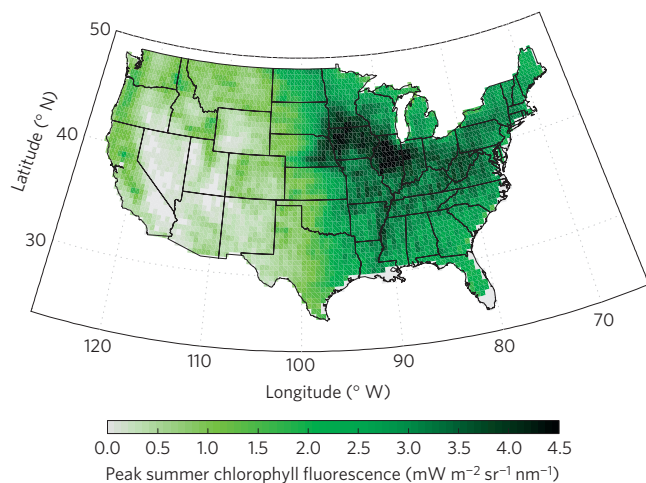


Figure 1 | Peak rates of summer chlorophyll fluorescence⁴⁹ in the US Midwest are the highest observed anywhere on the planet. Average monthly chlorophyll fluorescence from the GOME-2 satellite is calculated using data for 2007–2012. Maximum monthly average fluorescence achieved during June–August is plotted for every grid cell. Over the Midwest, summer maxima are typically achieved in July. A global comparison is presented in Supplementary Fig. 11.

Crops tend to exhibit less reduction in stomatal conductance at high vapour pressure deficits relative to natural vegetation²⁹, with the notable exception of recently developed varieties with high water

use efficiency³⁰, suggesting conversion may particularly influence hot days. Our analysis, however, indicates that those areas with the greatest rates of land conversion over this time period are not associated with statistically significant cooling (Fig. 3a,b, $P > 0.05$). In contrast, those areas with the greatest cropland abandonment have, on average, experienced significant cooling ($P < 0.05$), contrary to the proposed connection with temperatures. Greatest rates of cropland conversion since 1910 average approximately 3% of grid cell area per decade, whereas in the late 1800s rates reached 10–20% of grid cell area per decade over the Midwest³¹, indicating that cropland conversion more greatly influenced nineteenth-century temperature changes.

Increased irrigation is associated with cooling

Observational and modelling studies have demonstrated the ability of irrigation to cool surface temperatures through greater soil moisture and evapotranspiration^{12–16}. Our analysis shows a significant cooling effect associated with increases in irrigated area calculated from agricultural census data (Fig. 3c,d). Weather stations in counties with increases in irrigated area of greater than 10% of county area per decade show significant cooling. Where irrigation increases have been largest, such as in eastern Nebraska with trends greater than 7% of county area per decade, 95th percentile temperatures have cooled at a rate of 0.30 °C per decade ($P < 0.01$). Significant cooling associated with increased irrigation is, however, generally found only in Nebraska, Arkansas and the western US; and amounts only to around 11% of the 134 million hectares cooling at rates of at least 0.2 °C per decade (area calculations are performed using Voronoi polygons associated with each

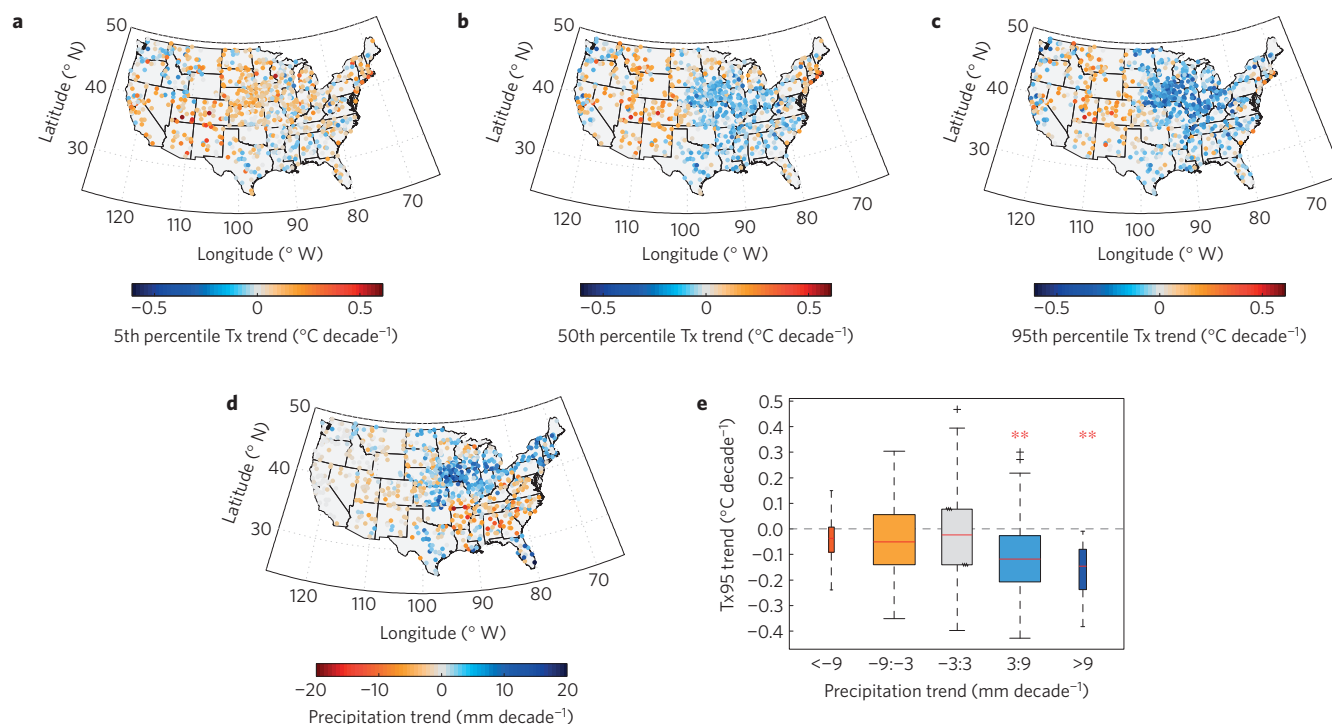


Figure 2 | The centennial trend towards cooler daily maximum temperatures during the summer in the Midwest is strongest for the hottest days of the year, and is accompanied by elevated precipitation across much of the region. **a–c**, Quantile regression trends for 1910–2014 for the 5th (**a**), 50th (**b**) and 95th (**c**) percentile of June, July and August (JJA) daily maximum temperatures (Tx). **d**, Trends in total JJA precipitation. **e**, Weather stations, and their corresponding trends in JJA 95th percentile daily maximum temperatures (Tx95), are grouped according to trends in JJA precipitation. Median temperature trends for each subset of data are indicated by horizontal red lines. Dashed vertical whiskers show the range of temperature trends, with any values exceeding 1.5× the interquartile range indicated by cross marks. Asterisks indicate that mean cooling across stations is significant for a given subset at $P < 0.05$ (single) or $P < 0.01$ (double) using a double-sided test. Trends are shown excluding the Dust Bowl (1930s) and the period of maximum aerosol-induced cooling in the eastern US (1970s–1990s), demonstrating cooling in the absence of these influences. Boxes are area-weighted (Supplementary Information), and the bin overlapping with zero has been collapsed to 1/5 of the original width.

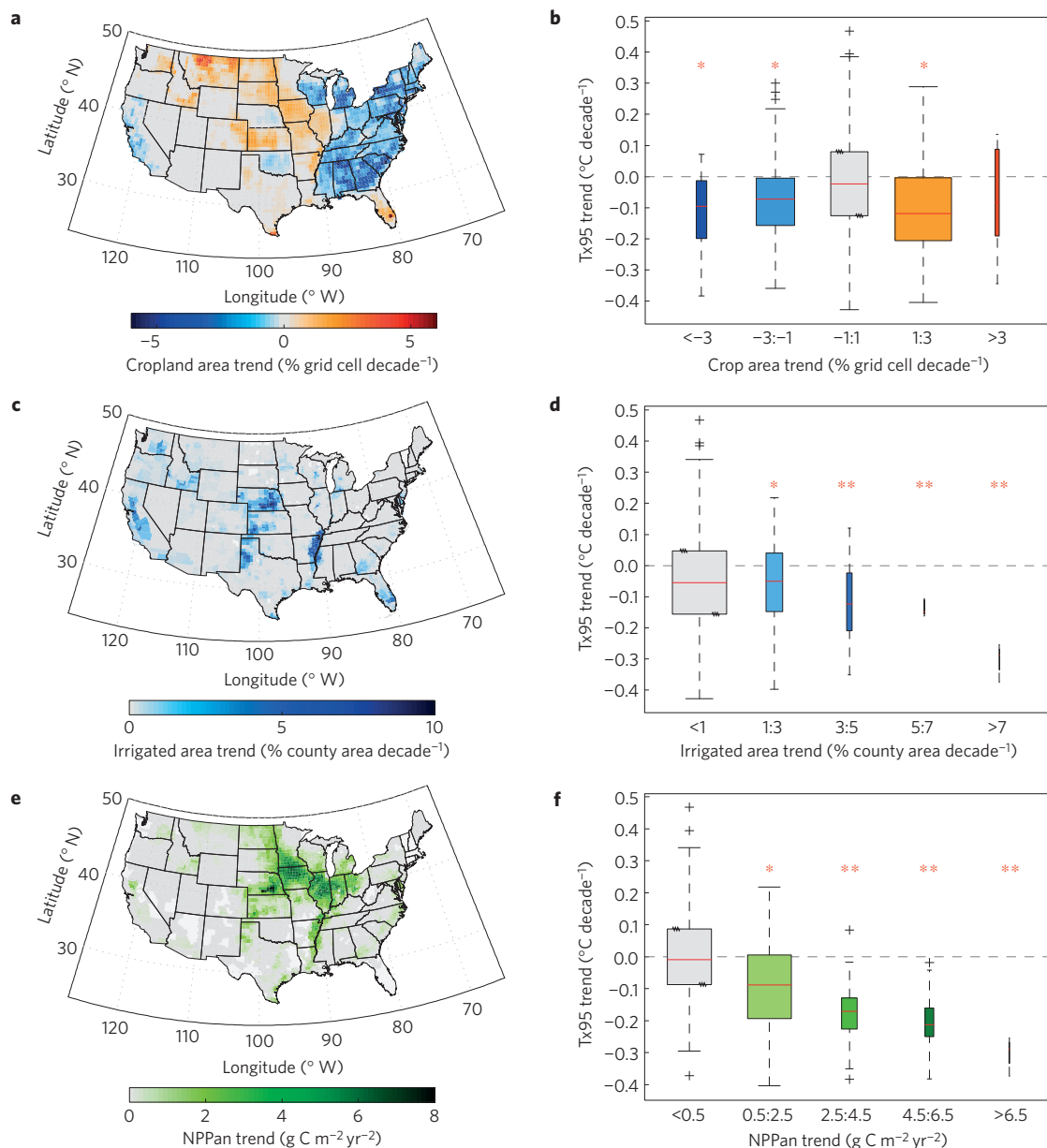


Figure 3 | Strong correspondence is found between the cooling pattern and cropland intensification, whereas increased irrigation correlates with cooling over a subset of the area and land cover change to cropland exhibits no association. a, Trends in total cropland area for 1910–2014. **b**, Weather stations, and their corresponding trends in JJA 95th percentile daily maximum temperatures (Tx95), are grouped according to trends in total cropland area. **c–f**, Similar to **a,b**, but for irrigated area (**c,d**), and area-normalized crop net primary productivity (NPPan) (**e,f**) calculated from USDA survey data on areas and yields of 12 major summer crop types. Median temperature trends for each subset of data are indicated by horizontal red lines. Dashed vertical whiskers show the range of temperature trends, with any values exceeding $1.5 \times$ the interquartile range indicated by cross marks. Asterisks indicate that mean cooling across stations is significant for a given subset at $P < 0.05$ (single) or $P < 0.01$ (double) using a double-sided test. Trends in 95th percentile maximum temperatures are calculated as in Fig. 2, excluding the Dust Bowl and the period of maximum aerosol-induced cooling. Boxes are area-weighted (Supplementary Information), and bins overlapping with zero have been collapsed to 1/5 of the original width. The lightest grey counties for **c** and **e** indicate insufficient data.

weather station). Comparison of local cooling to local irrigation trends seems appropriate, as high-resolution model results indicate that the cooling effects associated with irrigation are localized¹³.

Cropland intensification is associated with cooling

Another major change over the past century has been the marked intensification of crop management and productivity. Several lines of evidence suggest that changes in management practices, cultivar properties and crop choice associated with more intensive land use would lead to elevated evapotranspiration rates, even for

rainfed croplands. Widespread increases in fertilization have largely alleviated nitrogen stress, which can otherwise reduce photosynthetic rates, stomatal conductance, leaf area index and root development^{32,33}, resulting in decreased magnitude³⁴ and duration³⁴ of peak evapotranspiration in the field. Evapotranspiration can also be affected by the frequency of fallow¹⁷, planting density³⁵ and shifts in crop types³⁶. In particular, there has been a transition towards more maize and soybean acreage at the expense of hay and shorter-season³⁷ oats (Supplementary Fig. 2). Increased adoption of no-till systems can prevent early-season soil evaporation and

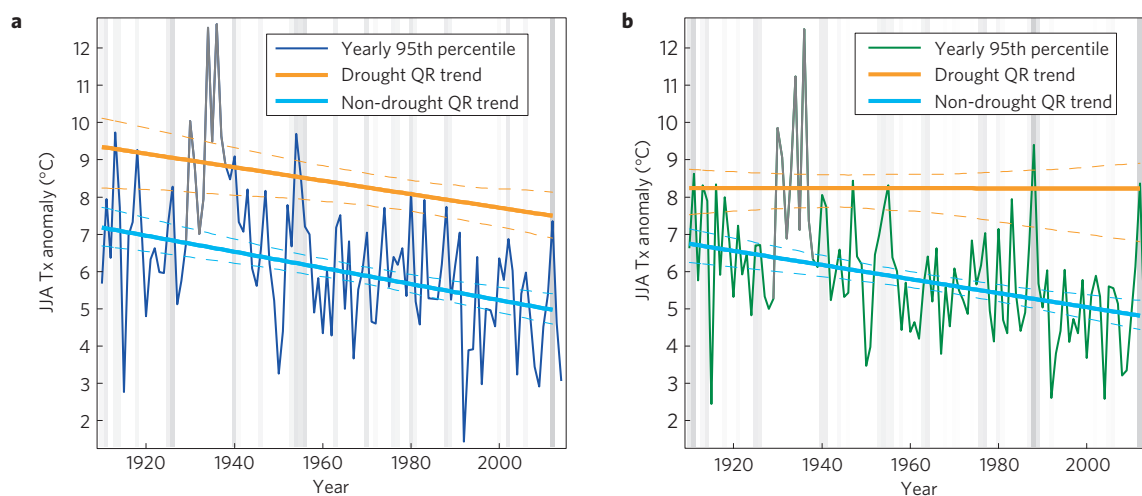


Figure 4 | Rainfed areas show reductions in extreme temperatures only when sufficient moisture is available, increasing the temperature difference between drought and non-drought years, whereas irrigated areas are cooler regardless of drought status. a, b, Trends in 95th percentile June–August temperature anomalies (relative to the 1910–2014 average) for areas with large growth in irrigation ($\geq 5\%$ county area decade $^{-1}$) (**a**) and rainfed areas with large increases in NPPan ($\geq 3 \text{ g C m}^{-2} \text{ yr}^{-2}$, excluding stations with $>10\%$ irrigated area) (**b**). To illustrate the dependence of the temperature trend on moisture availability in rainfed areas, we show quantile regression (QR) trends for 95th percentile temperatures calculated during drought (orange line) and non-drought (light blue line) conditions. The 10th percentile of the self-calibrated Penman–Monteith Palmer drought severity index⁴⁷ (available to 2012) is used as a drought index, and daily anomaly data are subset at each station according to drought category in a given month. Trends are using daily data across all selected stations, and yearly 95th percentile temperature anomalies are calculated within each subset. Dashed lines indicate 90% confidence intervals calculated using a bootstrap resampling of years (1,000 \times), and grey shading in the background corresponds to the proportion of daily observations experiencing drought conditions in a given year. Note that we have excluded the Dust Bowl, as dust from land degradation is thought to have concentrated and amplified temperature increases from drought⁵⁰ during this anomalous event (see Supplementary Fig. 5 for sensitivity analyses).

conserve water for transpiration³⁸. Evidence from the crop breeding literature also suggests that rooting and transpiration characteristics of cultivars have changed over time in ways that allow for greater evapotranspiration potential (Supplementary Information).

The inference of trends towards greater potential for evapotranspiration is supported by observations of increased specific and relative humidity across the Midwest during summer^{39,40}, a positive evapotranspiration trend in the region inferred from a Mississippi basin water balance⁴¹, and the presence of a smaller diurnal temperature range over US croplands as compared with forested landscapes⁴². The cooling influence of elevated evapotranspiration on temperatures is expected to be most pronounced for high-temperature days when evaporative demand is the greatest⁴³, consistent with observed temperature trends.

To quantitatively evaluate whether changes in agricultural intensity correspond with the observed spatial pattern and magnitude of cooling across the US, we calculate an index of agricultural intensity since 1910 using county-level USDA (US Department of Agriculture) survey records of crop harvested area and yield. We use 12 major summer crop types and calculate crop carbon fixation by county using conversion factors relating crop yield to whole-plant carbon content. Adjusting for county area provides estimates of area-normalized net primary productivity (NPPan) in grams of carbon fixed per year and per unit area ($\text{g C m}^{-2} \text{ yr}^{-1}$). This metric accounts for land use influences on evapotranspiration through integrating the effects of crop type, harvested area, and productivity. Examples of county-specific NPPan data are shown in Supplementary Fig. 3.

Changes in agricultural intensity closely correspond to the pattern of Midwest cooling (Fig. 3e,f and Supplementary Tables 1 and 2). Counties with local trends in NPPan greater than $4.5 \text{ g C m}^{-2} \text{ yr}^{-1}$ show a highly significant cooling in 95th percentile temperatures of 0.22°C per decade ($P < 0.01$), and counties with sequentially lower trends in NPPan show correspondingly smaller rates of cooling. These findings are

robust to the exclusion of locations with $>10\%$ irrigated area, and support our hypothesis of increased evapotranspiration potential in high-productivity croplands cooling high temperatures. Increasing NPPan is associated with seven times more land area undergoing cooling of at least 0.2°C per decade than irrigation. It is remarkable that cooling has occurred despite increased atmospheric carbon dioxide, which is associated with lower rates of transpiration, increased water use efficiency⁴⁴, and—along with other greenhouse gases—general surface warming.

Increased precipitation also favours greater evapotranspiration and may itself be influenced by evapotranspiration. Recent work in the Canadian Prairies has shown that increased crop evapotranspiration is correlated with greater specific humidity and precipitation¹⁷; such changes to the surface energy balance can favour deep convection and increase the frequency and severity of precipitation events^{17,45}. Evapotranspiration of irrigated water would also lead to increased precipitation and moisture recycling, and it has previously been suggested that Midwest growing-season precipitation increases may partly be attributed to irrigation^{28,46}.

Other possible influences on temperature trends

Despite strong evidence for the influence of intensification on cooling, it is important to consider two other potential influences. Simulations of tropospheric aerosol emissions, whose rates peaked near the 1980s, indicate widespread cooling over the eastern US, particularly in autumn^{21,22}. To further examine the importance of aerosols for growing-season temperatures, we compute trends since 1980 and, despite diminishing aerosol influence, again find a pattern of cooling similar to longer-term trends (Supplementary Fig. 1). Other research pointed to a relationship between cooling and an increase in the North Atlantic Oscillation index⁴¹ between 1960 and 1995, but the reversal of this trend since 1995 (Supplementary Fig. 4) and our additional calculations showing sustained cooling over recent decades suggest that the North Atlantic Oscillation has little influence on the hottest growing-season temperatures.

Interaction of cooling trends and moisture supply

A further test of our hypothesis is possible through examination of high temperatures during drought, during which the capacity for elevated evapotranspiration would not be realized. Months of daily temperature anomalies from counties exhibiting a trend in NPPan of $>2.5 \text{ g C m}^{-2} \text{ yr}^{-2}$ are subset for drought and non-drought conditions as defined by the self-calibrated Penman–Monteith Palmer drought severity index⁴⁷, and a regional temperature trend is fitted to each subset for the 95th percentile using quantile regression (Fig. 4 and Supplementary Fig. 5). As expected, regions with large growth in irrigation ($\geq 5\%$ county area per decade) show cooling regardless of drought status (Fig. 4a). In rainfed areas there is also a cooling trend during non-drought conditions, but no such trend appears during drought conditions (Fig. 4b). We infer that inadequate soil moisture eliminates the ability to achieve greater rates of evapotranspiration. These results suggest a greater degree of drought-induced warming in recent years, as baseline cooler temperatures revert to historically hot conditions. Differences between drought and non-drought trends reach approximately 3°C during 1988 and 2012.

Interpretation and future research

Our preferred explanation for improvements in Midwestern growing conditions is that the general intensification of agriculture, including regional increases in irrigation, causes cooling through increased evapotranspiration, especially on the hottest days. Increased evapotranspiration then also increases precipitation and overall rates of water recycling. Such a scenario implies that historical improvements in yield are, in part, an unintentional benefit of climate moderation brought about by other steps taken to improve yield. In future work it will be useful to explicitly simulate climate responses to increased potential evapotranspiration. Such simulation will benefit from continued improvement of land surface models with respect to representation of phenology, transpiration, irrigation, multiple crop types, and variable management intensity.

Few other locations on Earth have such extensive areas of summer crops, and none is more productive during the peak of the growing season than the US Midwest⁴⁸, suggesting that Midwest climate experienced especially strong forcing from land surface modification. Despite the favourable shifts that have occurred, it is unclear whether such trends can be sustained given rising greenhouse gas concentrations and limits to agricultural intensification imposed by water availability. Analyses of historical land use and climate data in other major agricultural regions, along with modelling of future land use scenarios and associated climate responses, are needed to understand the generalizability and persistence of intensification–cooling relationships.

Methods

Methods and any associated references are available in the [online version of the paper](#).

Received 21 May 2015; accepted 11 September 2015;
published online 12 October 2015

References

- Tilman, D., Balzer, C., Hill, J. & Befort, B. L. Global food demand and the sustainable intensification of agriculture. *Proc. Natl Acad. Sci. USA* **108**, 20260–20264 (2011).
- Lobell, D. B., Schlenker, W. & Costa-Roberts, J. Climate trends and global crop production since 1980. *Science* **333**, 1–9 (2011).
- Schlenker, W. & Roberts, M. J. Nonlinear temperature effects indicate severe damages to US crop yields under climate change. *Proc. Natl Acad. Sci. USA* **106**, 15594–15598 (2009).
- Butler, E. E. & Huybers, P. Adaptation of US maize to temperature variations. *Nature Clim. Change* **3**, 68–72 (2012).
- Lobell, D. B. *et al.* The critical role of extreme heat for maize production in the United States. *Nature Clim. Change* **3**, 1–5 (2013).
- Twine, T. E., Kucharik, C. J. & Foley, J. A. Effects of land cover change on the energy and water balance of the Mississippi River basin. *J. Hydrometeorol.* **5**, 640–655 (2004).
- Oleson, K. W., Bonan, G. B., Levis, S. & Vertenstein, M. Effects of land use change on North American climate: Impact of surface datasets and model biogeophysics. *Clim. Dynam.* **23**, 117–132 (2004).
- Bonan, G. B. Frost followed the plow: Impacts of deforestation on the climate of the United States. *Ecol. Appl.* **9**, 1305–1315 (1999).
- Davin, E. L., Seneviratne, S. I., Ciais, P., Olliso, A. & Want, T. Preferential cooling of hot extremes from cropland albedo management. *Proc. Natl Acad. Sci. USA* **111**, 9757–9761 (2014).
- Luyssaert, S. *et al.* Land management and land-cover change have impacts of similar magnitude on surface temperature. *Nature Clim. Change* **4**, 389–393 (2014).
- Jeong, S. J. *et al.* Effects of double cropping on summer climate of the North China Plain and neighbouring regions. *Nature Clim. Change* **4**, 615–619 (2014).
- Lobell, D. B., Bonfils, C. J., Kueppers, L. M. & Snyder, M. A. Irrigation cooling effect on temperature and heat index extremes. *Geophys. Res. Lett.* **35**, L09705 (2008).
- Harding, K. J. & Snyder, P. K. Modeling the atmospheric response to irrigation in the Great Plains. Part I: General impacts on precipitation and the energy budget. *J. Hydrometeorol.* **13**, 1667–1686 (2012).
- Mahmood, R. *et al.* Impacts of irrigation on 20th century temperature in the northern Great Plains. *Glob. Planet. Change* **54**, 1–18 (2006).
- Adegoke, J. O., Pielke, R. A. Sr, Eastman, J., Mahmood, R. & Hubbard, K. G. Impact of irrigation on midsummer surface fluxes and temperature under dry synoptic conditions: A regional atmospheric model study of the US High Plains. *Mon. Weath. Rev.* **131**, 556–564 (2003).
- Lu, Y., Jin, J. & Kueppers, L. M. Crop growth and irrigation interact to influence surface fluxes in a regional climate-cropland model. *Clim. Dynam.* **117**, 1–17 (2015).
- Betts, A. K., Desjardins, R., Worth, D. & Cerkowinski, D. Impact of land use change on the diurnal cycle climate of the Canadian Prairies. *J. Geophys. Res.* **118**, 11996–12011 (2013).
- Fall, S. *et al.* Impacts of land use land cover on temperature trends over the continental United States: Assessment using the North American Regional Reanalysis. *Int. J. Climatol.* **30**, 1980–1993 (2010).
- Pielke, R. A. Sr *et al.* An overview of regional land-use and land-cover impacts on rainfall. *Tellus B* **59B**, 587–601 (2007).
- Pielke, R. A. Sr *et al.* Land use/land cover changes and climate: Modeling analysis and observational evidence. *WIREs Clim. Change* **2**, 828–850 (2011).
- Leibensperger, E. M. *et al.* Climatic effects of 1950–2050 changes in US anthropogenic aerosols—Part 1: Aerosol trends and radiative forcing. *Atmos. Chem. Phys.* **12**, 3333–3348 (2012).
- Leibensperger, E. M. *et al.* Climatic effects of 1950–2050 changes in US anthropogenic aerosols—Part 2: Climate response. *Atmos. Chem. Phys.* **12**, 3349–3362 (2012).
- Portmann, R. W., Solomon, S. & Hegerl, G. C. Spatial and seasonal patterns in climate change, temperatures, and precipitation across the United States. *Proc. Natl Acad. Sci. USA* **106**, 7324–7329 (2009).
- Robinson, W. A., Ruedy, R. & Hansen, J. E. General circulation model simulations of recent cooling in the eastern United States. *J. Geophys. Res.* **107**, 4748 (2002).
- Meehl, G. A., Arblaster, J. M. & Branstator, G. Mechanisms contributing to the warming hole and the consequent US east–west differential of heat extremes. *J. Clim.* **25**, 6394–6408 (2012).
- Goldstein, A. H., Koven, C. D., Heald, C. L. & Fung, I. Y. Biogenic carbon and anthropogenic pollutants combine to form a cooling haze over the southeastern United States. *Proc. Natl Acad. Sci. USA* **106**, 8835–8840 (2009).
- Kunkel, K. E., Liang, X.-Z., Zhu, J. & Lin, Y. Can CGCMs simulate the twentieth-century ‘warming hole’ in the central United States? *J. Clim.* **19**, 4137–4153 (2006).
- DeAngelis, A. *et al.* Evidence of enhanced precipitation due to irrigation over the Great Plains of the United States. *J. Geophys. Res.* **115**, 1–14 (2010).
- Franks, P. J. & Farquhar, G. D. A relationship between humidity response, growth form and photosynthetic operating point in C3 plants. *Plant Cell Environ.* **22**, 1337–1349 (1999).
- Gilbert, M. E., Holbrook, N. M., Zwieniecki, M. A., Sadok, W. & Sinclair, T. R. Field confirmation of genetic variation in soybean transpiration response to vapor pressure deficit and photosynthetic compensation. *Field Crops Res.* **124**, 85–92 (2011).
- Ramankutty, N. & Foley, J. A. Estimating historical changes in global land cover: Croplands from 1700 to 1992. *Glob. Biogeochem. Cycles* **13**, 997–1027 (1999).

32. Jones, J. W., Zur, B. & Bennett, J. M. Interactive effects of water and nitrogen stresses on carbon and water vapor exchange of corn canopies. *Agric. For. Meteorol.* **38**, 113–126 (1986).
33. Chapin, F. S. III, Walter, C. H. & Clarkson, D. T. Growth response of barley and tomato to nitrogen stress and its control by abscisic acid, water relations and photosynthesis. *Planta* **173**, 352–366 (1988).
34. Rudnick, D. R. & Irmak, S. Impact of nitrogen fertilizer on maize evapotranspiration crop coefficients under fully irrigated, limited irrigation, and rainfed settings. *J. Irrig. Drain. Eng.* **140**, 1–15 (2014).
35. Jiang, X. *et al.* Crop coefficient and evapotranspiration of grain maize modified by planting density in an arid region of northwest China. *Agric. Water Manage.* **142**, 135–143 (2014).
36. Allen, R. G., Pereira, L. S., Raes, D. & Smith, M. *Crop Evapotranspiration—Guidelines for Computing Crop Water Requirements* (Food and Agriculture Organization of the United Nations, 1998).
37. USDA NASS *Usual Planting and Harvest Dates for US Field Crops* 1–51 (United States Department of Agriculture, 1997).
38. Gallaher, R. N. Soil moisture conservation and yield of crops no-till planted in rye. *Soil Sci. Soc. Am. J.* **41**, 145–147 (1977).
39. Brown, P. J. & DeGaetano, A. T. Trends in US surface humidity, 1930–2010. *J. Appl. Meteorol. Climatol.* **52**, 147–163 (2013).
40. Sandstrom, M. A., Lauritsen, R. G. & Changnon, D. A central-US summer extreme dew-point climatology (1949–2000). *Phys. Geogr.* **25**, 191–207 (2004).
41. Milly, P. & Dunne, K. A. Trends in evaporation and surface cooling in the Mississippi River basin. *Geophys. Res. Lett.* **28**, 1219–1222 (2001).
42. Bonan, G. B. Observational evidence for reduction of daily maximum temperature by croplands in the Midwest United States. *J. Clim.* **14**, 2430–2442 (2001).
43. Seneviratne, S. I. *et al.* Investigating soil moisture–climate interactions in a changing climate: A review. *Earth Sci. Rev.* **99**, 125–161 (2010).
44. Leakey, A. D. B. *et al.* Elevated CO₂ effects on plant carbon, nitrogen, and water relations: Six important lessons from FACE. *J. Experim. Bot.* **60**, 2859–2876 (2009).
45. Raddatz, R. L. Anthropogenic vegetation transformation and the potential for deep convection on the Canadian prairies. *Can. J. Soil Sci.* **78**, 657–666 (1998).
46. Harding, K. J. & Snyder, P. K. Modeling the atmospheric response to irrigation in the Great Plains. Part II: The precipitation of irrigated water and changes in precipitation recycling. *J. Hydrometeorol.* **13**, 1687–1703 (2012).
47. Dai, A. Characteristics and trends in various forms of the Palmer Drought Severity Index during 1900–2008. *J. Geophys. Res.* **116**, D12115 (2011).
48. Guanter, L. *et al.* Global and time-resolved monitoring of crop photosynthesis with chlorophyll fluorescence. *Proc. Natl Acad. Sci. USA* **111**, E1327–E1333 (2014).
49. Joiner, J. *et al.* Global monitoring of terrestrial chlorophyll fluorescence from moderate spectral resolution near-infrared satellite measurements: Methodology, simulations, and application to GOME-2. *Atmos. Meas. Tech. Discuss.* **6**, 3883–3930 (2013).
50. Cook, B. I., Miller, R. L. & Seager, R. Amplification of the North American 'Dust Bowl' drought through human-induced land degradation. *Proc. Natl Acad. Sci. USA* **106**, 4997–5001 (2009).

Acknowledgements

We thank F. Rockwell, T. Sinclair, L. Mickley, K. Harding, T. Twine, P. Snyder and C. O'Connell for helpful discussions. We thank N. Ramankutty for sharing the updated historical cropland data set. This work was supported by the National Science Foundation (Hydrologic Sciences grant 1521210) and by a fellowship from the Harvard University Center for the Environment to N.D.M.

Author contributions

N.D.M., P.H., N.M.H. and E.E.B. conceived of the study. A.R., K.A.M., M.T. and P.H. developed the precision-decoding necessary to enable quantile regression. N.D.M. led data analysis, with assistance from P.H., E.E.B. and A.R. N.D.M., P.H. and N.M.H. led writing and interpretation of the results, with assistance from E.E.B., A.R., K.A.M. and M.T.

Additional information

Supplementary information is available in the [online version of the paper](#). Reprints and permissions information is available online at www.nature.com/reprints. Correspondence and requests for materials should be addressed to N.D.M.

Competing financial interests

The authors declare no competing financial interests.

Methods

Land use and land cover trends. Changes to crop net primary productivity (NPP) are assessed using data from the USDA National Agricultural Statistics Service's annual surveys⁵¹. We collect county- and state-level crop harvested area and yield data for 19 major crop types (only state-level data are available for New England). A subset of 12 crop types are identified with a summer growing season³⁷ and adequate spatial and temporal resolution: maize, soybean, spring wheat, durum wheat, oats, barley, peanuts, pima cotton, upland cotton, rice, sorghum and dry bean. We note that a relatively small amount of barley and oats acreage is planted in the autumn and harvested in the spring³⁷, but that these are not reported separately in the USDA database. Winter wheat is excluded owing to the early harvest, whereas maize for silage, canola, sunflower (oil and non-oil) and hay (alfalfa and non-alfalfa) are excluded owing to data limitations. Crop areas and yields are converted to metric units using yield conversions from the USDA Economic Research Service⁵². We analyse area trends by state of all collected crop types in Supplementary Fig. 2.

From the yield data, NPP per harvested area (NPP_{ha}) is calculated using a standard technique to scale yield to carbon content:

$$\text{NPP}_{\text{ha}_{c,k,y}} = \frac{Y_{c,k,y} \text{DF}_c C}{\text{HI}_{c,y} \text{AF}_c}$$

where *c* is crop, *k* is political unit (county or state), *y* is year, *Y* is yield in t ha⁻¹, *DF* is the dry fraction of the crop, *C* is carbon content, *HI* is harvest index—the fraction of above-ground plant biomass allocated to harvested material, and *AF* is the fraction of biomass above ground. We use the harvest index, dry fraction, above-ground fraction and carbon content values of ref. 53, except for cotton values, which are from ref. 54. For crops for which we have reliable estimates on historical harvest indices, we assume a linearly varying harvest index between the historical and modern values from 1910 and 1980, with the modern harvest indices used after 1980. The starting harvest indices for historical cultivars^{55,56} are 0.33 for wheat, 0.37 for barley, and 0.3 for rice. We also use a historical harvest index for maize of 0.45 and a modern index of 0.5 based on ref. 55.

We then calculate an area-normalized NPP (NPP_{an}) by summing total carbon fixation (g C yr⁻¹) over all selected crops in a political unit and dividing by the total political unit area:

$$\text{NPP}_{\text{an}_{k,y}} = \sum_{c=1}^{12} \frac{\text{NPP}_{\text{ha}_{c,k,y}} \text{HA}_{c,k,y}}{\text{TA}_k}$$

where *HA* is harvested area (m²) and *TA* is the total area in the political unit (m²). The NPP_{an} metric integrates the influence of both the spatial extent and the productivity of major summer crops. A procedure to account for years with missing county-level data is outlined below. Simple linear regression is used to calculate the temporal trend in NPP_{an} for counties with data for at least 75% of years; trends are computed for irrigated area and total cropland area in a similar manner.

In the USDA database, some year by crop combinations (particularly early in the record) contain no county-resolved information. As NPP_{an} is a sum over all crops, intermittency in terms of which crops are available in a given year can bias the estimate. Thus, we use a two-part procedure for filling these gaps.

First, we determine cases where data on crop harvested area and yield are available at the state level but not at the county level. For these cases, we calculate the proportional allocation of harvested area between counties using the closest five years of county-resolved data, and state-level harvested area is allocated between the counties proportionally. We use state yield data when county yields are not available.

Second, remaining missing data points are identified and screened for three criteria: the crop of interest had at least ten area and yield observations throughout the record; within the closest ten years to the missing data point, the average NPP_{an} was at least 20 g C m⁻² yr⁻¹; and data are available for at least one other crop in the missing year. When these criteria are met, a regression is performed to estimate NPP_{an} for the missing data point based on the time series of NPP_{an} for other crops, year and year squared. The temporal trends are necessary to account for shifts in crop mix over the course of the record. Regression coefficients relating NPP_{an} of the selected crop to the other crops are constrained to be positive, and estimated NPP_{an} is required to be greater than or equal to zero.

Irrigated area trends are determined using data collected from historical US agricultural census reports⁵¹. We use county-, state- and national-level data to document and estimate historical irrigation. County-level data are used from the four most recent agricultural censuses (1997, 2002, 2007 and 2012). Before 1997, the average county-level spatial pattern from 1997–2012 (excluding any missing data) is scaled using state-level irrigated area data from 10 agricultural census reports back to 1940, available from the Census of Agriculture Historical Archive⁵⁷. Before 1940, national-level data from the 1940, 1935, 1930 and 1900 censuses are used to further scale the spatial pattern back to 1910. Irrigated acreage in 1910 is estimated by linearly interpolating between the 1900 and 1930 values.

Cropland area trends are determined using a gridded data set of agricultural census records³³. We use an updated version of the referenced data set that includes

data to 2007 (N. Ramankutty, personal communication). Temporary pasture is included in the definition of cropland for consistency with the UN Food and Agriculture Organization.

Climate trends and quantile regression of temperature data. We use weather station maximum temperature records from the Global Historical Climatology Network-Daily (GHCND) database⁵⁸. The GHCND station data are screened separately for each three-month season using four criteria. First, all observations having negative GHCND quality control flags are excluded. A spatial subset then retains only stations in the continental US. We then screen for temporal completeness, and only stations that are at least 80% complete for a given season over the duration of the time interval are retained. Each 5-year pentad is then examined, and stations are excluded if they are less than 75% complete in more than two years per pentad, ensuring that the maximum of 20% missing data are not overly concentrated in a particular span of time.

The GHCND data need to be corrected for double-rounding errors and finite-precision effects that can bias the results of quantile regression, and we use results from a precision-decoding algorithm⁵⁹ to mitigate these issues. Quantile regression assumes continuously distributed data, and we add a small amount of uniform jitter to the data to approximate the underlying distribution. The jitter amplitude is equal to the observational precision inferred from precision-decoding⁵⁹. Without these corrections, quantile regression trend estimates would be substantially biased towards zero.

Quantile regression⁶⁰ temperature trends are computed for each weather station, with sensitivity to trend start dates and data exclusions (for example, the Dust Bowl) shown in Supplementary Fig. 1. Trends for the 95th percentile of June–August temperatures, excluding the Dust Bowl (1930s) and the period of maximum aerosol-induced cooling (1970s–1990s), are compared against local land use and land cover trends for Fig. 3 by using the cropland area trend from the closest grid cell and the irrigation and NPP_{an} changes for the relevant county or, in the case of New England, state. Grid cell values of the self-calibrated Penman–Monteith Palmer drought severity index⁴⁷ for July and August are associated with weather stations in a similar manner to group observations by drought status for Fig. 4. Trends in 95th percentile temperatures by season are shown in Supplementary Figs 6 and 7.

Precipitation trends are assessed for GHCND stations with high-quality temperature data. Similar to the temperature data, we exclude any observations with negative quality flags. Average precipitation per day is calculated by season. Years missing >50% of days are removed, and trends are calculated only for stations with at least 75% coverage. Precipitation trends by season are shown in Supplementary Figs 8 and 9. A time series of precipitation trends for those stations shown in Fig. 3 is presented in Supplementary Fig. 10.

Statistical analyses. The significance of average quantile regression trends across stations grouped by precipitation and local land use (Figs 2d and 3b,d,f and Supplementary Table 1) is analysed using a bootstrapping approach that accounts for spatial autocorrelation. We resample years with replacement, selecting all stations in a given year to preserve spatial autocorrelation. We find the mean quantile regression trend across stations and repeat 1,000 times, generating an empirical distribution of mean trends from which a two-sided *p* value is determined. We also calculate point-wise correlations between temperature and land use change trends that are shown in Supplementary Table 2.

Assigning physical area to weather stations. A Voronoi tessellation is used to assign a zone of nearby physical area to weather stations (Supplementary Fig. 12). All weather stations meeting quality criteria are included. Polygon areas from the Voronoi tessellation are used to calculate the widths of the boxplots presented in the main text. However, land use characteristics are from the local grid cell or county in which the weather station is located.

References

- USDA NASS *National Agricultural Statistics Service* (United States Department of Agriculture, 2014); http://www.nass.usda.gov/Quick_Stats
- USDA ERS *Weights, Measures, and Conversion Factors for Agricultural Commodities and Their Products* 1–77 (United States Department of Agriculture, 1992).
- Monfreda, C., Ramankutty, N. & Foley, J. A. Farming the planet: 2. Geographic distribution of crop areas, yields, physiological types, and net primary production in the year 2000. *Glob. Biogeochem. Cycles* **22**, GB1022 (2008).
- Lobell, D. B. *et al.* Satellite estimates of productivity and light use efficiency in United States agriculture, 1982–98. *Glob. Change Biol.* **8**, 722–735 (2002).
- Hay, R. Harvest index: A review of its use in plant breeding and crop physiology. *Ann. Appl. Biol.* **126**, 197–216 (1995).
- Riggs, T. J. *et al.* Comparison of spring barley varieties grown in England and Wales between 1880 and 1980. *J. Agric. Sci.* **97**, 599–610 (1981).

57. *Census of Agriculture Historical Archive* (United States Department of Agriculture, 2014); <http://agcensus.mannlib.cornell.edu>
58. Menne, M. J., Durre, I., Vose, R. S., Gleason, B. E. & Houston, T. G. An overview of the global historical climatology network-daily database. *J. Atmos. Ocean. Technol.* **29**, 897–910 (2012).
59. Rhines, A., Tingley, M. P., McKinnon, K. A. & Huybers, P. Decoding the precision of historical temperature observations. *Q. J. R. Meteorol. Soc.* 1–11 (2015).
60. Koenker, R. & Bassett, G. Jr Regression quantiles. *Econometrica* **46**, 33–50 (1978).